

# Attempted endocytosis of nano-environment produced by colloidal lithography by human fibroblasts

Matthew J. Dalby,<sup>a,\*</sup> Catherine C. Berry,<sup>a</sup> Mathis O. Riehle,<sup>a</sup> Duncan S. Sutherland,<sup>b</sup> Hossein Agheli,<sup>b</sup> and Adam S.G. Curtis<sup>a</sup>

<sup>a</sup>Centre for Cell Engineering, Institute of Biomedical and Life Sciences, University of Glasgow, Glasgow G12 8QQ, UK

<sup>b</sup>Department of Applied Physics, Chalmers University of Technology, Gothenburg 41296, Sweden

Received 14 November 2003, revised version received 29 January 2004

## Abstract

Control of the cells' nanoenvironment is likely to be important in the future of cell and tissue engineering. Microtopography has been shown to provide cues to cells that elicit a large range of cell responses, including control of adhesion, morphology, apoptosis and gene regulations. Now, researchers are focusing on nanotopography as techniques such as colloidal and electron beam lithography and polymer demixing have become available. In this study, human fibroblast response to nanocolumns (160-nm high, 100-nm diameter, 230-nm centre–centre spacing) produced by colloidal lithography are considered. Using electron microscopy and immunofluorescence to image the cytoskeleton, clathrin and dynamin, it was observed that the cells try to endocytose the nanocolumns. It also appeared that a small population of the cells changed to unusual morphologies with macrophage-like processes and highly disrupted cytoskeleton. These observations could have implications for nanomaterials science in areas such as cell transfection and drug delivery.

© 2004 Elsevier Inc. All rights reserved.

**Keywords:** Endocytosis; Nanoenvironment; Colloidal lithography; Human fibroblasts

## Introduction

Tissue engineering aims to restore the function of damaged tissues by engineering cell function using scaffold materials [1,2]. At present, many of these materials possess uncharacterised surface topographies and this may significantly limit the clinical success of the material. Materials that have structured micro- and nanodesigns may provide a way of eliciting responses that could be exploited for research tools and medical materials.

Micron-scale topographies have been shown to induce changes in cell adhesion, morphology, motility and gene expression [3–8] (please refer to Ref. [9] for a recent review). These surfaces certainly appear to have potential in areas such as cell guidance to sites of tissue organisation [10,11] and cell differentiation [8]. Cells will, however, also be surrounded by nanoscale cues that may also be

used to enhance and control cell response. Only recently, however, have the manufacturing techniques for nanofabrication been available on a scale sufficient for cell experiments. Such techniques include electron-beam lithography [12], polymer demixing [13] and colloidal lithography [14–16].

In this report, the response of a major tissue-forming cell, the fibroblast, is investigated in relation to 160-nm-high, 100-nm-diameter, nanocolumns produced by colloidal lithography. For this technique, an array of monodispersed nanocolloids are electrostatically assembled on a substrate and then used as a template for etching into the substrate material [14,16]. The result of which are cylindrical columns sculpted into the bulk polymer.

It seems likely that filopodia are one of the cell's main sensory tools. Gustafson and Wolpert [17] first described filopodia in living cells in 1961. They observed mesenchymal cells migrating up the interior wall of the blastocoelic cavity in sea urchins and noted that the filopodia produced appeared to explore the substrate. This led them to speculate that they were being used to gather spatial information by the cells [18].

\* Corresponding author. Centre for Cell Engineering, Institute of Biomedical and Life Sciences, University of Glasgow, Joseph Black Building, Glasgow G12 8QQ, UK. Fax: +44-141-3303730.

E-mail address: [m.dalby@bio.gla.ac.uk](mailto:m.dalby@bio.gla.ac.uk) (M.J. Dalby).

Filopodia have been associated with the sensing of chemoattractant gradients (haptotaxis) [19,20] and sensing of chemically different islands within polymers [21]. When considering filopodial sensing of topography, neuronal growth cone filopodia have been described as sensing and then aligning cells to microgrooves [3,22,23]. Similar observations have also been made for fibroblasts sensing microgrooves [4].

Once a cell locates a suitable feature using the filopodia presented on the leading edge, lamellipodia are formed that move the cell to the desired site. These actions require G-protein signalling and the actin cytoskeleton; specifically, Cdc42 is required for filopodial assembly [24]. Cells lacking Cdc42 cannot sense chemotactic gradients and simply migrate in a random manner [25]. This, again, presents compelling evidence for filopodial involvement in cell sensing.

As well as looking into filopodial sensing of nanotopography, this report also focuses on cell endocytosis (ingestion of extracellular matter by cells). Such uptake by cells can be roughly divided into three mechanisms: pinocytosis, endocytosis and phagocytosis; the divides, however, are not clear. Phagocytosis is traditionally considered to be the uptake of large particulates, for example bacteria by macrophages. Endocytosis routinely occurs in all cell types and is associated with uptake of proteins, perhaps the best characterised being the transferrin–iron complex [26]. Pinocytosis is considered to be involved with fluid-phase uptake, often occurring with endocytosis. Clathrin coats the vesicles formed during small-particle endocytosis, but is not involved with all types of endocytosis. Here, we consider clathrin-mediated endocytosis [26,27].

To investigate filopodial sensing and endocytosis, scanning and transmission electron microscopies (SEM and TEM) have been used. The cytoskeletal elements actin, tubulin and vimentin and the proteins clathrin, dynamin and Rac have been observed by fluorescence microscopy.

## Materials and methods

### Materials

The starting substrates for fabrication of all samples was bulk PMMA. The PMMA substrates were precut into  $8 \times 8$  mm squares using a diamond saw (Loadpoint). The 1-mm-thick substrates were precut to a depth of 600  $\mu\text{m}$  from the backside. Colloidal lithography was used to modify the surface of the polymer producing nanostructured features. This approach is described in detail elsewhere [14,16], but in brief utilises electrostatically assembled dispersed monolayers of colloidal particles as masks for pattern transfer into substrate materials. In this work, the substrate materials were pretreated with a light oxygen plasma (0.25 T 50w RF 120s Batchtop) followed by electrostatic self-assembly of a multilayer of polyelectrolytes [poly(diallyldimethylammo-

nium chloride) (PDDA, MW 200,000–350,000, Aldrich), poly(sodium 4-styrenesulfonate) (PSS, MW 70000, Aldrich) and aluminium chloride hydroxide (ACH, Reheis)]. Subsequent assembly of a colloidal mask (sulphate-modified polystyrene colloid  $107 \pm 5$  nm IDC USA) from aqueous solution followed by drying resulted in a dispersed colloidal monolayer which has short-range order, but no long-range order.

The pattern of the colloidal mask was transferred into the bulk polymer using a combination of vertical and angled argon ion bombardment (250 eV 0.2 mA/cm<sup>2</sup> 600 s from 15° from vertical followed by 840 s from vertical CAIBE Ion Beam System-Oxford Ionfab); etching was continued until the particles were completely removed resulting in cylindrical pillars. Fig. 1 shows an AFM height image of the resultant structures (tapping mode DI dimensions 3000 sharpened Silicon oxide tip NT-MDT). During the etching process, the surface of the polymer is oxidised and cross-linked with the argon ions penetrating only relatively short distances into the polymer and modifying only a thin outer layer (5–7 nm). Flat control substrates with matched surface chemistry (characterised by XPS, data not shown here) were fabricated by subjecting flat PMMA substrates with no assembled particles to argon ion bombardment. The resultant surfaces had roughness levels around 3–5 nm.

Samples for cell culture were snapped along the precut lines into  $8 \times 8$  mm squares and blown with nitrogen to remove any particulate contamination and presterilised in 70% ethanol. Fabrication and precleaning was carried out in a class 1000 clean room before packaging in air-tight boxes for transfer.

### Cell culture

Infinity™ telomerase immortalised human fibroblasts (hTERT-BJ1, Cloneteck Laboratories, Inc. USA) (passage 11) were seeded onto the test materials at a density of  $1 \times 10^4$  cells per sample in 1 ml of complete medium. The medium used was 71% Dulbecco's Modified Eagle's Medium (DMEM) (Sigma, Poole, UK), 17.5% Medium 199 (Sigma), 9% foetal calf serum (FCS) (Life Technologies, UK), 1.6% 200 mM L-glutamine (Life Technologies) and 0.9% 100 mM sodium pyruvate (Life Technologies). The cells were incubated at 37°C with a 5% CO<sub>2</sub> atmosphere.

### Immunofluorescence and cytoskeletal observation

After 4 days of culture (approximately 60% confluence), cells were fixed in 4% formaldehyde/PBS, with 1% sucrose at 37°C for 15 min. The samples were washed with PBS, and a permeabilising buffer (10.3 g sucrose, 0.292 g NaCl, 0.06 g MgCl<sub>2</sub>, 0.476 g HEPES buffer, 0.5 ml Triton X, in 100 ml water, pH 7.2) was added at 4°C for 5 min. The samples were then incubated at 37°C for 5 min in 1% BSA/PBS, followed by the addition of either an anti-clathrin, anti-Dynamin, anti-rac, anti-vimentin or anti- $\beta$  tubulin primary

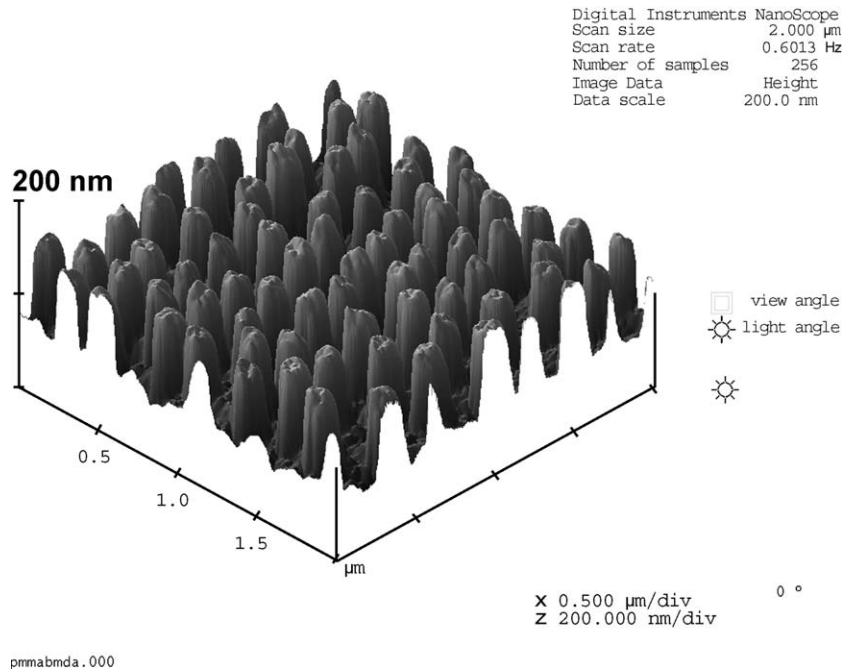


Fig. 1. Atomic force microscopical image of the 160-nm-high nanocolumns.

antibody [1:100 in 1% BSA/PBS monoclonal anti-human antibody raised in mouse (IgG1), h-vin1 (vinculin), V9 (vimentin), tub 2.1 (tubulin), Sigma, 23A8 (rac), Hudy-1 (dynamin), Upstate Biotech or clathrin from Biogenesis] for 1 h (37°C) (Table 1). Rhodamine-conjugated phalloidin was added for the duration of this incubation (1:100 in 1% BSA/PBS, Molecular Probes, OR, USA). The samples were next washed in 0.5% Tween 20/PBS (5 min  $\times$  3). A secondary, biotin-conjugated antibody [1:50 in 1% BSA/PBS, monoclonal horse anti-mouse (IgG), Vector Laboratories, Peterborough, UK] was added for 1 h (37°C) followed by washing. A FITC-conjugated streptavidin third layer was added (1:50 in 1% BSA/PBS, Vector Laboratories, Peterborough, UK) at 4°C for 30 min, and given a final wash. Samples were then viewed by fluorescence microscope (Zeiss Axiovert 200 M).

Table 1  
Reasons for choice of antigens

Antigen	Reason
Actin (microfilaments)	Possible involvement in vesicle movement [28].
Tubulin (microtubules)	Involvement in vesicle guidance and recycling [29].
Dynamin	Microtubule-associated GTPase associated with pinching the vesicle from the cell membrane [29].
Clathrin	Coats the vesicles formed during endocytosis [27].
Rac	G-protein associated with lamellae formation in cells [30].
Vimentin (intermediate filaments)	Associated with mechanotransduction associated with changes in cell shape [31].

#### Transmission electron microscopy

After 4 weeks of culture, cells were fixed with 1.5% glutaraldehyde (Agar, UK) buffered with 0.1 M sodium cacodylate (Agar) for 1 h. Cells were postfixed with 1% osmium tetroxide, dehydrated in a series of alcohols. Once dehydrated the samples were embedded in Spurr's resin (TAAB, UK) and polymerised at 70°C for 18 h. Ultrathin sections were cut, stained with uranyl acetate (2% aq.) and lead citrate, and viewed with a Zeiss TEM.

#### Scanning electron microscopy

Cells were fixed with 1% glutaraldehyde (Sigma) buffered in 0.1 M sodium cacodylate (Agar) (4°C, 1 h) after a 4-day incubation period. The cells were then post-fixed in 1% osmium tetroxide (Agar) and 1% tannic acid (Agar) was used as a mordant, then dehydrated through a series of alcohol concentrations. The final dehydration was in hexamethyl-disilazane (Sigma). Once dry, the samples were sputter coated with gold before examination with a Hitachi S800 or S4700 field emission SEM.

## Results

Atomic force microscopical observation of the substrates revealed that nanocolumns had been produced. The columns were measured to be 160 nm in height, 100 nm in diameter, and had approximately 230 nm centre–centre spacing (Fig. 1).

Fibroblasts cultured on the planar controls had normal *in vitro* morphologies as shown by both SEM (Fig. 2A) and TEM (Fig. 2B). Cells on the nanocolumns, however, had many filopodia (Figs. 2C–F). These could be seen to interact with the nanocolumns both to the sides of (Figs. 2C–E) and underneath the cells (Fig. 2F and inset).

TEM examination of the lamellapodia on the nanocolumns showed that the cells were, in areas, internalising the columns (Figs. 3A–C). In many cases, nascent vesicles were observed in the proximity of these areas (Fig. 3A); in other cases, larger vesicles could be seen close by (Fig. 3C). SEM examination showed that in these areas, imprints of the nanocolumns could be seen in the lamellae (Fig. 3D).

Staining of actin showed that cells cultured on the nanocolumns had few stress fibres and that actin was mainly located cortically (Figs. 4A,C,E,G). On the planar controls, however, actin was highly organised, with stress fibres observed through the cytoplasm of the fibroblasts (Figs. 4B,D,F,H). Microtubules were seen to be clearly organised in cells on the controls, radiating to the cell periphery from the tubulin organising centre (Fig. 4B). Whilst tubulin was still seen to be clearly organised in fibroblasts on the nanocolumns, the amount of tubulin appeared to be reduced, i.e., less dense in appearance (Fig. 4A). Vimentin intermediate filaments were observed to be clearly organised in

cells grown on the planar controls (Fig. 4H). Vimentin was less distinct, however, in cells on the nanocolumns (Fig. 4G). In these cells, vimentin was mainly observed close to the cell nucleus, with little vimentin found in the cell lamellae. Vimentin could, however, be observed in filopodia (Fig. 4G, inset).

Clathrin staining in fibroblasts on the flat controls showed only diffuse staining, representing only background levels of endocytosis (Fig. 4F). In cells on the nanocolumns, concentrated clathrin localisation was observed at the cell peripheries, and it appeared that clathrin could also be seen in the cell cytoplasm (Fig. 4E). Dynamin was seen to be present in basal levels in fibroblasts on the controls (Fig. 4D), but increased levels were observed in cells on the nanocolumns (Fig. 4C). In these cells, increased dynamin was seen in lamellae and appeared to be associated to microtubules (Fig. 4C).

A small population of cells cultured on the nanocolumns appeared to take on almost macrophage-like morphologies, forming large cavities reminiscent of the pseudopodial pits used for phagocytosis (Figs. 5A,B). In these cells, the actin cytoskeleton was seen to be highly disrupted, but clearly involved in the formation of these cavities (Figs. 5C,E). Tubulin was seen to be disrupted in the main cell body, but clearly organised in the cytosol joining the cavities to the

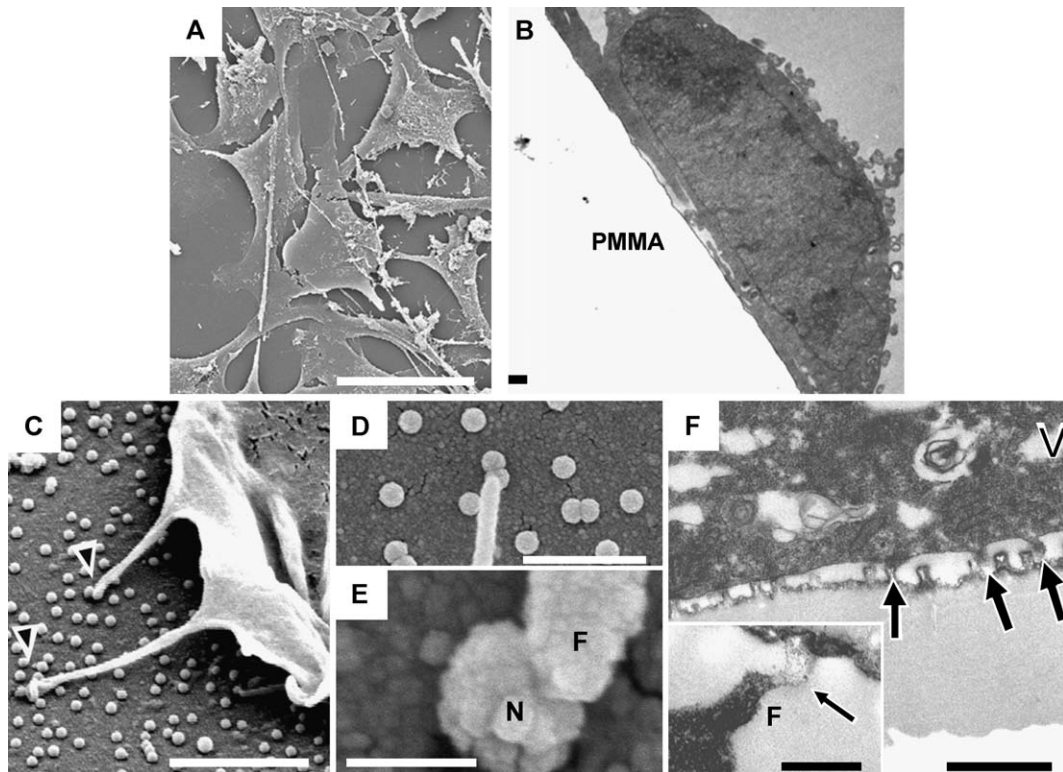


Fig. 2. Electron microscopical images of fibroblast filopodia interacting with nanocolumns. (A) Scanning electron micrograph (scale bar = 40  $\mu$ m) and (B) transmission electron micrograph (scale bar = 500 nm) showing fibroblasts with normal morphology growing on planar control (scale bar = 40  $\mu$ m). (C) Scanning electron micrograph of filopodia interacting with nanocolumns (arrowheads) (scale bar = 1  $\mu$ m, imaged at 45° tilt). (D) As with C, but imaged directly overhead (scale bar = 500 nm). (E) High-magnification scanning electron micrograph showing a filopodium (F) interacting with a nanocolumn (N) (scale bar = 100 nm). (F) Transmission electron micrograph of filopodia underneath the cells interacting with nanocolumns (arrows) (scale bar = 500 nm), inset at higher magnification (F = filopodia) (scale bar = 200 nm).

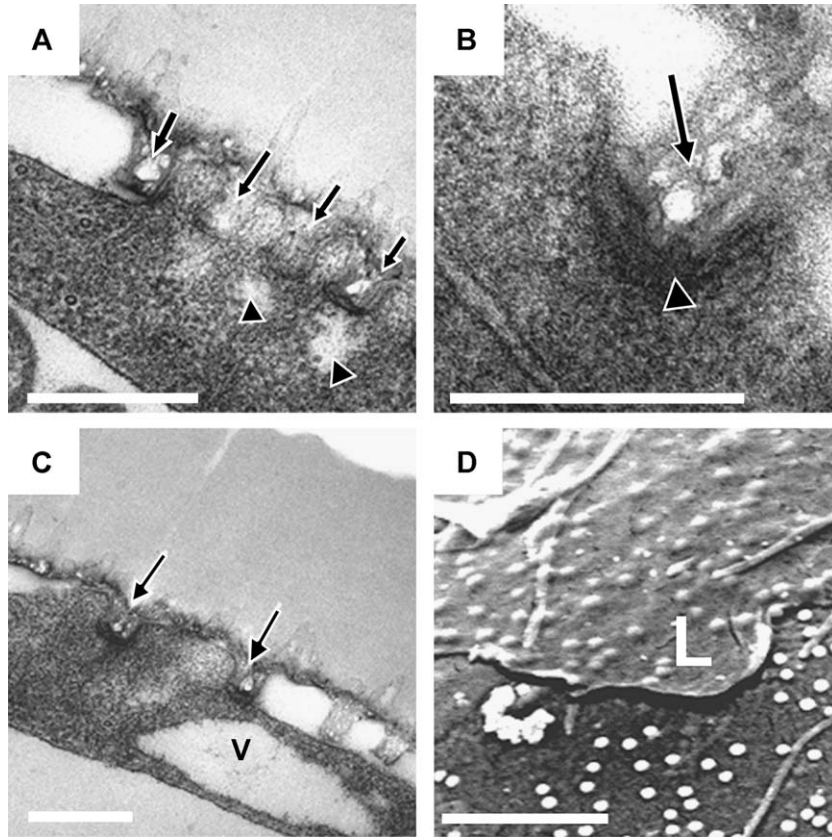


Fig. 3. Images of fibroblasts attempting to endocytose nanocolumns. (A–C) Transmission electron micrographs of fibroblast lamellae enveloping the nanocolumns (scale bar = 400 nm). (A) Formation of nascent vesicles (arrowheads) forming in close relation to the nanocolumns (arrows). (B) Formation of an endocytotic pit (arrowhead) forming around a nanocolumn (arrow). (C) A larger vesicle (V) in close proximity of the nanocolumns (arrows). (D) Scanning electron micrograph showing that the shape of the nanocolumns were clearly visible under the thin cell lamellae (L) (scale bar = 1.5  $\mu$ m).

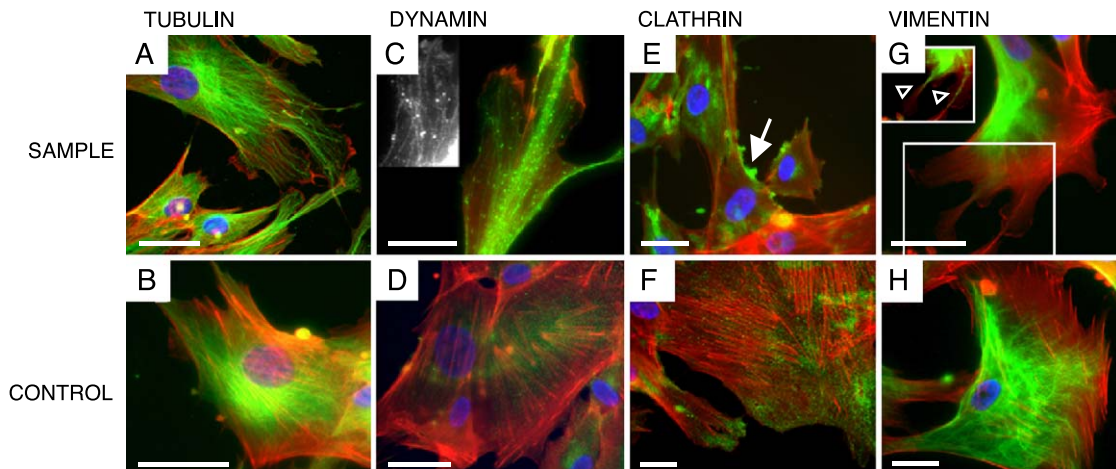


Fig. 4. Fluorescent images showing attempted endocytosis of nanocolumns. (A) Organised tubulin cytoskeleton (green) on the nanocolumns; denser tubulin is present in cells on planar control (B). (C) Dynamin (green) was clearly present, and possibly associated to microtubules (inset), in the cell lamellae, whereas on control (D) only background levels of dynamin were observed. (E) High levels of clathrin (green) accumulating at the cell peripheries on the nanocolumns (arrow), compared to only diffuse staining observed in cells on the planar controls (F). (G) Poorly organised vimentin (green) in fibroblasts on the nanocolumns. Inset shows that vimentin (contrast enhanced) was sparsely found in the lamellae, but was observed in the cells filopodia (arrowheads). (H) Well-organised vimentin in fibroblasts on the planar controls. All images show actin (red in all images) to be more clearly organised in the cells on the planar controls. The cells cultured on the nanocolumns have many less stress fibres. (Note: in all images, blue = nucleus, red = actin; scale bar = 20  $\mu$ m).

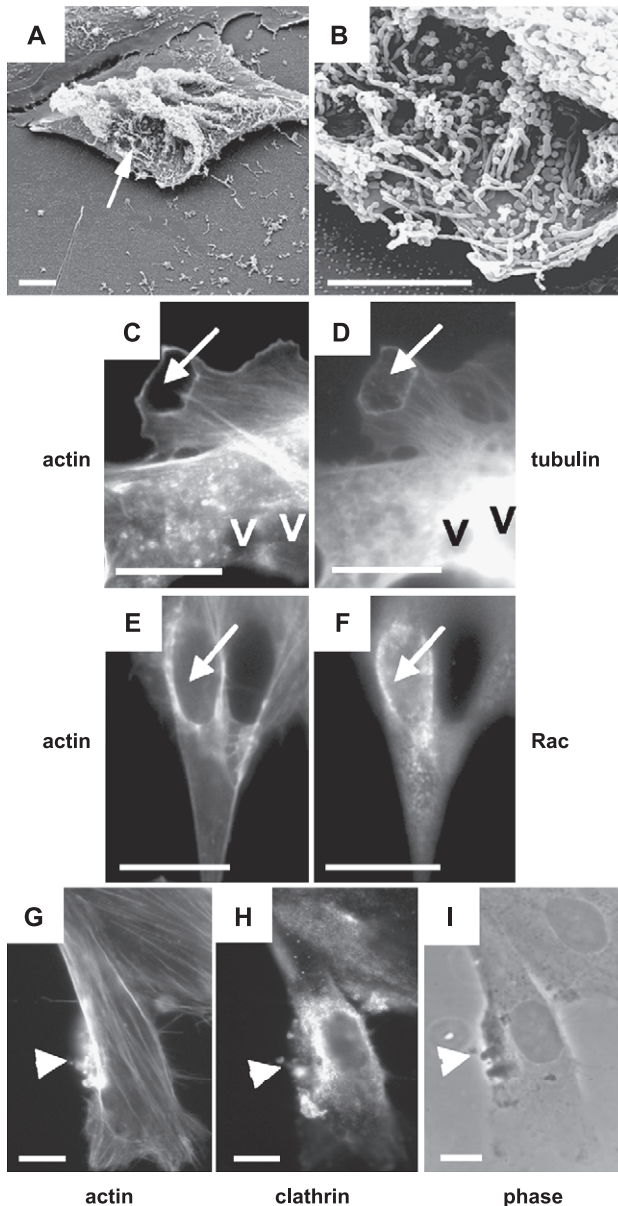


Fig. 5. Fibroblasts with macrophage-like phagocytotic pseudopodia. (A,B) Scanning electron micrographs of pseudopodial openings (arrow) (scale bar = 10  $\mu$ m). (C) In these cells, actin was badly disrupted, but was located to the outer ring of the pseudopod (arrow) (scale bar = 25  $\mu$ m). (D) Tubulin in the same cell was seen to be badly disrupted in the cell body, but clearly organised coming from the pseudopod (arrow) (scale bar = 25  $\mu$ m, V = vesicle). (E) Poorly organised actin in a cell protrusion was again seen to be involved in pseudopod formation. (F) Rac located to the opening in the same cell. (G–I) Actin (G) and clathrin (H), for the same cell (scale bar = 25  $\mu$ m). The cell appears to be badly disrupted (I), with high levels of attempted endocytosis to the left hand side (arrowheads).

main cell body (Fig. 4D). The G-protein Rac (involved in lamellipodium formation [23]) was also seen to be localised to these sites (Fig. 5F).

Some cells with intermediate morphologies were also observed on the columns. Phase images of these cells showed that they had invaginated membranes (Fig. 5I), that

actin was becoming disrupted at these points (Fig. 5G) and that clathrin levels were high at these points (Fig. 5H).

## Discussion

It was seen that initially filopodia were observed to sense and interact with the columns. Some of the filopodia, as in Fig. 2D, appeared to push against the nanocolumns, leading to flattening of the filopodia ends.

The results suggest that once the fibroblasts have located the nanocolumns, they attempt to endocytose them. Clathrin-mediated endocytosis is a process whereby a cell ingests nanosized material. All cells will have constant, background, endocytosis. Steps in cell clathrin-mediated endocytosis include membrane invagination, clathrin coated pit formation, coated pit sequestration, detachment of the newly formed vesicle via action of the small GTPase dynamin and finally movement of this new endocytic compartment away from the plasma membrane into the cytosol [32,33]. Thus, the localisation of clathrin at the cell peripheries, where TEM also showed the fibroblasts surrounding the nanocolumns, indicates that the fibroblasts were attempting to internalise the columns. Whilst empty vesicles were often observed near the columns, no evidence of internalised, removed or damaged structures was found. The columns forming part of the bulk PMMA were presumably too strongly attached to the surface.

This is in agreement with several recent studies. Wood et al. [34] looked at the underside of epitenon cells grown on 50-nm-diameter gold colloids attached to a silicon surface by amilnosaline, and in their study, the cells were not able to move the colloids. Whilst in other studies using polymeric particles coated in thin metallic films, no ability for the cells to remove the structures was observed [35,36].

In further support of the cells trying to endocytose the nanocolumns, dynamin was also observed to be located to these regions. Dynamin is a microtubule-associated small GTPase and is involved in pinching the clathrin-coated vesicles so as to allow internalisation (see Ref. [37] for a review of dynamin). Essentially, dynamin binds and hydrolyses GTP, resulting in a net motive force used to sever membrane tubules [38,39].

Involvement of the cytoskeleton in endocytosis is less clear. Actin is being tied into the movement dynamics of endocytotic vesicles, but further proof is being sought [32,33,40]. Within this study, little association of actin/clathrin and actin/dynamin was observed in most of the cells expressing these proteins. In fact, cells on the nanocolumns had less clearly organised actin cytoskeletons. Vimentin was also seen to be poorly organised in cells on the nanocolumns, and appeared to be absent from regions of lamellae. Tubulin, however, was observed to be clearly organised in fibroblasts on the nanocolumns, although quantity appeared to be reduced. Organisation of microtubules is required for endocytosis with dynamin being

microtubule associated [41]. Stable tubulin arrangement is also required for recycling of endocytotic vesicles [42].

The cytoskeleton is involved in cell support and mechanotransduction. In our recently submitted work, we have shown reduced cell spreading and changes in adhesion characteristics and morphology of focal contacts, with contacts formed on nanocolumns being smaller than those formed on planar control. Focal contacts are important in cell signalling (see Ref. [43] for a review). Recent thinking is that focal contacts are also considered to be important in supporting the cytoskeleton and cell shape through the formation of tensegrity structures [44,45]. Thus, reduced cell spreading and focal adhesion formation may be causing the reduced cytoskeletal organisation observed here.

Changes in adhesion morphology have also been observed recently on other nanotopographies. Fibroblasts cultured on 13-nm-high, 260-nm-wide islands (random arrangement, produced by polymer demixing) showed increases in the number of adhesions expressed and increased actin and tubulin organisation [46]. Epithelial cells cultured on nanopits with a 150-nm diameter (orthogonal arrangement, produced by electron beam lithography) showed a marked reduction in cell adhesion; cells that were adhered had small focal adhesions and poorly organised actin cytoskeleton [47]. Epithelial cell adhesion morphology has also been shown to conform to the size of nanogrooves, with focal adhesion width increasing with groove width (groove dimensions from 70-nm width and 400-nm pitch up to 1.9- $\mu$ m width and 4- $\mu$ m pitch) [48]. Also, in older studies with microgrooved topographies, changes in adhesion morphologies have also been observed, with alignment of focal contacts and cytoskeletons in macrophages and fibroblasts [6,49] along the grooves.

The combination of these results demonstrates that topography may strongly influence the formation of focal adhesions and subsequent formation of cytoskeleton, and that this may in turn alter the ability of cells to spread. Here, it is seen that actin and vimentin are poorly organised in cells cultured on the nanocolumns. Thus, in agreement with the cellular tensegrity model, where microtubules act as load-bearers, intermediate filaments as tensile stiffeners and microfilaments acting to anchor the tensegrity unit and apply prestress to it [50,51], the cells on the nanocolumns are less well spread with less-defined cytoskeletons compared to those on control. The exception, in this case, being the microtubules, which are clearly organised due to the requirements for endocytosis.

An interesting observation was the very small population of poorly spread fibroblasts with disrupted cytoskeletons and pseudopodial, ‘macrophage-like’ processes [52]. The actin and tubulin cytoskeletons were, however, seen to be well organised around the pseudopodia-like cavity, suggesting that the cells were attempting to ingest from the external environment. Rac was also seen to locate to these processes, localising with actin, hence driving the cell to produce the processes.

Similar disruption of fibroblast cytoskeleton has been previously seen in fibroblasts that have endocytosed large quantities of magnetic nanoparticles. These cells were observed to contain large vesicles and very diffuse microfilaments and microtubules [53], reminiscent of the cells shown in Fig. 4 in this report. Uptake of high levels of nanoscale particles has also been shown to disrupt macrophage cytoskeleton and function [54]. Thus, in this study, it appears that cells only need the external stimuli of particles/columns for this disruption to take place.

This report shows that control of the cells nanoenvironment can lead to increased levels of endocytosis. In this environment, the cells are responding as if they are reacting both to a fixed topography, by altering adhesions and cytoskeleton, and to free nanoparticles by inducing endocytosis.

### Acknowledgments

Matthew Dalby is a BBSRC David Phillips Fellow. This work was supported by the EU framework V grant QLK3-CT-2000-01500 (Nanomed). We would like to thank the Glasgow University Integrated Microscopy Facility for help with EM preparation and CDW Wilkinson for his interesting discussion.

### References

- [1] R. Langer, J.P. Vacanti, *Tissue engineering*, *Science* 260 (1993) 920–9266.
- [2] A. Persidis, *Tissue engineering*, *Nat. Biotechnol.* 17 (1999) 508–510.
- [3] P. Clark, P. Connolly, A.S.G. Curtis, J.A.T. Dow, C.D.W. Wilkinson, Topographical control of cell behaviour: simple step cues, *Development* 99 (1987) 439.
- [4] P. Clark, P. Connolly, A.S.G. Curtis, J.A.T. Dow, C.D.W. Wilkinson, Topographical control of cell behaviour: II. Multiple grooved substrata, *Development* 108 (1990) 635–644.
- [5] B. Wojciak-Stothard, A. Curtis, W. Monaghan, K. MacDonald, C. Wilkinson, Guidance and activation of murine macrophages by nanometric scale topography, *Exp. Cell Res.* 223 (1996) 426–435.
- [6] S. Britland, H. Morgan, B. Wojciak-Stothard, M. Riehle, A. Curtis, C. Wilkinson, Synergistic and hierarchical adhesive and topographic guidance of BHK cells, *Exp. Cell Res.* 228 (1996) 313–325.
- [7] C.S. Chen, M. Mrksich, S. Huang, G.M. Whitesides, D.E. Ingber, Geometric control of cell life and death, *Science* 276 (1997) 1425–1428.
- [8] M.J. Dalby, M.O. Riehle, S.J. Yarwood, C.D.W. Wilkinson, A.S.G. Curtis, Nucleus alignment and cell signalling in fibroblasts: response to a micro-grooved topography, *Exp. Cell Res.* 283 (2003) 274–282.
- [9] G.A. Abrams, A.I. Teixeira, P.F. Nealey, C.J. Murphy, The effects of substratum topography on cell behaviour, in: A.K. Dillow, A. Lowman (Eds.), *Biomimetic Materials and Design: Interactive Bioartificial Strategies*, Tissue Engineering, and Drug Delivery, Marcel Dekker, New York, 2002.
- [10] B. Wojciak, J. Crossan, A.S.G. Curtis, C.D.W. Wilkinson, Grooved substrata facilitate in vitro healing of completely divided flexor tendons, *J. Mater. Sci.: Mater. Med.* 6 (1995) 266–271.
- [11] C.C. Berry, G. Campbell, A. Spadicino, M. Robertson, A.S.G. Cur-

- tis, The influence of microscale topography on fibroblast attachment and motility, *Biomaterials* (in press).
- [12] C.D.W. Wilkinson, M. Riehle, M. Wood, J. Gallagher, A.S.G. Curtis, The use of materials patterned on a nano- and micro-metric scale in cellular engineering, *Mater. Sci. Eng., C* 19 (2002) 263–269.
- [13] S. Affrossman, G. Henn, S.A. O'Neill, R.A. Pethrick, M. Stamm, Surface topography and composition of deuterated polystyrene-poly (bromostyrene) blends, *Macromolecules* 29 (1996) 5010–5016.
- [14] F.A. Denis, P. Hanarp, D.S. Sutherland, Y.F. Dufrière, Fabrication of nanostructured polymer surfaces using colloidal lithography and spin-coating, *Nanoletters* 2 (2002) 1419–1425.
- [15] M.A. Wood, M.O. Riehle, C.D.W. Wilkinson, Patterning colloidal nanotopographies, *Nanotechnology* 13 (2002) 605–609.
- [16] P. Hanarp, D.S. Sutherland, J. Gold, B. Kasemo, Control of nanoparticle film structure for colloidal lithography, *Colloids Surf., A* 214 (2003) 23–36.
- [17] T. Gustafson, L. Wolpert, Studies on the cellular basis of morphogenesis in the sea urchin embryo: directed movements of primary mesenchyme cells in normal and vegetated larvae, *Exp. Cell Res.* 24 (1961) 64–79.
- [18] W. Wood, P. Martin, Structures in focus-filopodia, *Int. J. Biochem. Cell Biol.* 34 (2002) 726–730.
- [19] M. Ueda, Y. Sako, T. Tanaka, P. Devreotes, T. Yanagida, Single-molecule analysis of chemotactic signalling in *Dictyostelium* cells, *Science* 294 (2001) 864–867.
- [20] M. Iijima, P. Devreotes, Tumor suppressor PTEN mediates sensing of chemoattractant gradients, *Cell* 109 (2002) 599–610.
- [21] M.J. Dalby, L. Di Silvio, N. Gurav, B. Annaz, M.V. Kayser, W. Bonfield, Optimizing HAPEX™ topography influences osteoblast response, *Tissue Eng.* 8 (2002) 453–467.
- [22] A.M. Rajniecek, C.D. McCaig, Guidance of CNS growth cones by substratum grooves and ridges: effects of inhibitors of the cytoskeleton, calcium channels and signal transduction pathways, *J. Cell Sci.* 110 (1997) 2915–2924.
- [23] E. Stepien, J. Stanisiz, W. Korohoda, Contact guidance of chick embryo neurons on single scratches in glass and on underlying aligned human skin fibroblasts, *Cell Biol. Int.* 23 (1999) 105–116.
- [24] A.A. Schmitz, E.E. Govek, B. Bottner, L. Van Aelst, Rho GTPases: signaling, migration, and invasion, *Exp. Cell Res.* 261 (2002) 1–12.
- [25] G.E. Jones, W.E. Allen, A.J. Ridley, The Rho GTPases in macrophage motility and chemotaxis, *Cell Adhes. Commun.* 6 (1998) 237–245.
- [26] C.C. Berry, A.S.G. Curtis, Functionalisation of magnetic nanoparticles for applications in biomedicine, *J. Phys. D: Appl. Phys.* 36 (2003) R198–R206.
- [27] S.M. Tse, W. Furuya, E. Gold, A.D. Schreiber, K. Sandvig, R.D. Inman, S. Grinsein, Differential role of actin, clathrin and dynamin in Fc gamma receptor mediated endocytosis and phagocytosis, *J. Biol. Chem.* 278 (2002) 3331–3338.
- [28] S.R. da Costa, C.T. Okamoto, S.F. Hamm-Alvarez, et al., Actin microfilaments—the many components, effectors and regulators of epithelial cell endocytosis, *Adv. Drug Delivery Rev.* 14 (2003) 1359–1383.
- [29] R.B. Vallee, P.M. Okamoto, The regulation of endocytosis: identifying dynamin's binding partners, *Trends Cell Biol.* 5 (1995) 43–47.
- [30] S.L. Rogers, U. Wiedemann, N. Stuurman, R.D. Vale, Molecular requirements for actin-based lamella formation in *Drosophila* S2 cells, *J. Cell Biol.* 162 (2003) 1079–1088.
- [31] I. Holloway, M. Kayser, D.A. Lee, D.L. Bader, G. Bentley, M.M. Knight, Increased presence of cells with multiple elongated processes in osteoarthritic femoral head cartilage, *Osteoarthr. Cartil.* 12 (2004) 17–24.
- [32] B. Qualmann, M.M. Kessels, R.B. Kelly, Molecular links between endocytosis and the actin cytoskeleton, *J. Cell Biol.* 150 (2000) F111–F116.
- [33] D.A. Schafer, Coupling actin dynamics and membrane dynamics during endocytosis, *Curr. Opin. Cell Biol.* 14 (2002) 76–81.
- [34] M.A. Wood, D.O. Meredith, G.Rh. Owen, Steps toward a model nanotopography, *IEEE Trans. Nanobiosci.* 1 (2002) 133–140.
- [35] A.-S. Andersson, F. Bäckhed, A. von Euler, A. Richter-Dahlfors, D.S. Sutherland, B. Kasemo, Nanoscale features influence epithelial cell morphology and cytokine production, *Biomaterials* 24 (2003) 3427–3436.
- [36] A.-S. Andersson, P. Olsson, U. Lidberg, D.S. Sutherland, The effects of discontinuous and continuous groove edges on cell shape and alignment, *Exp. Cell Res.* 288 (2003) 177–188.
- [37] J.E. Hinshaw, Dynamin and its role in membrane fission, *Annu. Rev. Cell Dev. Biol.* 16 (2000) 483–519.
- [38] R. Gagescu, J. Gruenberg, E. Smythe, Membrane dynamics in endocytosis: structure–function relationship, *Traffic* 1 (2000) 84–88.
- [39] M.A. McNiven, H. Cao, K.R. Pitts, Y. Yoon, The dynamin family of mechanoenzymes: pinching in new places, *TIBS* 25 (2000) 115–120.
- [40] L.M. Fujimoto, R. Roth, J.E. Heuser, S.L. Schmid, Actin assembly plays a variable, but not obligatory role in receptor-mediated endocytosis in mammalian cells, *Traffic* 1 (2000) 161–171.
- [41] H.S. Shpetner, R.B. Vallee, Dynamin is a GTPase stimulated to high levels of activity by microtubules, *Nature* 355 (1992) 733–735.
- [42] S.X. Lin, G.G. Gundersen, F.R. Maxfield, Export from pericentriolar endocytose recycling compartment to cell surface depends on stable, detyrosinated (Glu) microtubules and kinesin, *Mol. Biol. Cell* 13 (2002) 96–109.
- [43] K. Burridge, M. Chrzanowska-Wodnick, Focal adhesions, contractility, and signaling, *Annu. Rev. Cell Dev. Biol.* 12 (1996) 463–519.
- [44] D.E. Ingber, Tensegrity I. Cell structure and hierarchical systems biology, *J. Cell Sci.* 116 (2003) 1157–1173.
- [45] D.E. Ingber, Tensegrity II. How structural networks influence cellular information processing networks, *J. Cell Sci.* 116 (2003) 1397–1408.
- [46] M.J. Dalby, S.J. Yarwood, M.O. Riehle, H.J.H. Johnstone, S. Affrossman, A.S.G. Curtis, Increasing fibroblast response to materials using nano-topography: morphological and genetic measurements of cell response to 13-nm-high polymer demixed islands, *Exp. Cell Res.* 276 (2002) 1–9.
- [47] J.O. Gallagher, K.F. McGhee, C.D.W. Wilkinson, M.O. Riehle, Interaction of animal cells with ordered nano-topography, *IEEE Trans. Nanobiosci.* 1 (2002) 24–28.
- [48] A.I. Teixeira, G.A. Abrams, P.J. Bertics, C.J. Murphy, P.F. Nealy, Epithelial contact guidance on well-defined micro- and nanostructured substrates, *J. Cell Sci.* 116 (2003) 1881–1892.
- [49] E.T. den Braber, J.E. de Ruijter, L.A. Ginsel, A.F. von Recum, J.A. Jansen, Orientation of ECM protein deposition, fibroblast cytoskeleton and attachment complex components on silicone microgrooved surfaces, *J. Biomed. Mater. Res.* 40 (1998) 291–300.
- [50] D.E. Ingeber, Cellular tensegrity: defining new rules of biological design that govern the cytoskeleton, *J. Cell Sci.* 104 (1993) 613–627.
- [51] T. Charas, M.A. Horton, Single cell mechanotransduction and its modulation analyzed by atomic force microscope indentation, *Biophys. J.* 82 (2002) 2970–2981.
- [52] N. Morrissette, E. Gold, A. Ademer, The macrophage—a cell for all seasons, *Trends Cell Biol.* 9 (1999) 199–201.
- [53] C.C. Berry, S. Rudershausen, J. Teller, A.S.G. Curtis, The influence of elastin coated 520-nm and 20-nm-diameter nanoparticles on human fibroblasts in vitro, *IEEE Trans. Nanobiosci.* 1 (2002) 105–109.
- [54] W. Moller, T. Hofer, A. Ziesenis, E. Karg, J. Heyder, Ultrafine particles cause cytoskeletal dysfunctions in macrophages, *Toxicol. Appl. Pharmacol.* 182 (2002) 197–207.